Molecular Crystals and Liquid Crystals
Publication details, including instructions for authors and subscription information:
http://www.tandfonline.com/loi/gmcl20

Fluorescent Pattern Generation of Anthracene Polymers by Holographic Technique

Y. Kim [a], J. Kim [a] & E. Kim [a]

[a] Department of Chemical and Biomolecular Engineering, Yonsei University, Seongsanno, Seodaemun-gu, Seoul, South Korea

Version of record first published: 19 Apr 2010

To cite this article: Y. Kim, J. Kim & E. Kim (2010): Fluorescent Pattern Generation of Anthracene Polymers by Holographic Technique, Molecular Crystals and Liquid Crystals, 520:1, 223/[499]-230/[506]

To link to this article: http://dx.doi.org/10.1080/15421400903584481

Mol. Cryst. Liq. Cryst., Vol. 520: pp. 223/[499]–230/[506], 2010

ISSN: 1542-1406 print/1563-5287 online
DOI: 10.1080/15421400903584481

Fluorescent Pattern Generation of Anthracene Polymers by Holographic Technique

Y. KIM, J. KIM, AND E. KIM

Department of Chemical and Biomolecular Engineering, Yonsei University, Seongsanno, Seodaemun-gu, Seoul, South Korea

Photopolymer films were prepared from the mixture of acrylate monomer, binder, a visible light sensitive photo initiator, and fluorescent polymer (polyanthracene, PMAn), to generate the fluorescent patterns by holographic method. The transparent photopolymer films were yellow colored and having maximum fluorescent emission at visible range. The diffraction efficiency of the PMAn doped film with thickness of 100 μm was maximized to 50%. Fluorescent patterns in a submicron/micron scale were inscribed on the photopolymer film with a visible laser. As a result of the fluorescent grating patterns, the fluorescence of the film was highly enhanced compared to the unpatterned film.

Keywords Fluorescent pattern; holography; photo-patterning

1. Introduction

Patterning by laser interference technique such as holographic patterning has been interested as a new fabrication technique in multi-dimensional structure formation for polymer dispersed liquid, photochromic media, and photo polymerizable media [1–6]. In particular, photo sensitive polymer system in holography lithography has been exploited for diffractive elements and devices [7–15]. In this photo-polymerizable media, diffractive grating patterns were fabricated as a result of light initiating photo-polymerization at the brighter regions of the interference, by local and non local polymerization. Since the non-local polymerization followed by diffusion of monomers can be optically triggered and chemically amplified, patterns can be obtained with high homogeneity over larger area to afford simple pattering process.

Much report has been published to the surface relief gratings (SRG) of azo-functionalized or azo-doped polymers [16–19]. Despite of this, reports on emissive photopolymer films containing photo-polymerizable acrylates functional groups in the presence of fluorophore were rare [20]. We report here the formation of fluorescent pattern using the photopolymer system containing ethylene glycol phenyl ether acrylate and triazine diacrylate monomer (DT) [21]. As a fluorophore, we introduced methylene bridged poly-anthracene (PMAn) because of its high solubility in organic solution containing transparent binder [22].

Address correspondence to Eunkyoung Kim, Department of Chemical Engineering, Yonsei University, 134 Shinchon-dong, Seodaemun-gu, Seoul 120-749, South Korea. Tel.: 82-2-2123-5752; E-mail: eunkim@yonsei.ac.kr

2. Experiment

2.1. *Materials*

Ethylene glycol phenyl ether acrylate (PA) and polysulfone (PES, Mw = 35,000) were purchased from Aldrich. Bis (μ5–2,4 cyclopentadien-1-yl)-bis-[2,6-difluoro-3-(1Hpyrrol-1-yl) phenyl] titanium (Irgacure784) was purchased from Ciba Geigy and used as a photo radical initiator. The triazine dimethacrylate (DT) was synthesized from cyanuric chloride, according to the literature [21]. Chloroform and 1,1,2,2-tetrachloroethane (TCE) were purchased from Aldrich and used as solvent. The high molecular weight (Mw) PMAn having average Mw of 3650 ($M_w/M_n = 3.64$) was synthesized according to the method reported before [22]. The low Mw PMAn having average Mw of 1225 ($M_w/M_n = 1.22$) was synthesized similarly but with less initiator concentration [22].

2.2. *Preparation of Photopolymer Films for FL Pattern Formation*

PMAn was added to the mixture of photopolymer composition to fabricate the transparent fluorescent film. This visible light sensitive mixture consisted of PA and DT as monomers, polysulfone (PES, Mw = 35,000), a visible light sensitive photo initiator (Ig784), and PMAn as a fluorophore. There was no indication of polyanthracene dimerization under 491 nm or 514 nm because polyanthracene was dimerized only under UV light. The mixtures were dissolved well in a mixture of chloroform and TCE and then stirred under a dark place for 3 h. The photopolymer films from the monomer mixture of PA and DT afforded stable holographic recording as we reported before [23]. Thus all the holographic patterning was carried with the film containing an optimized content of DT. The optimized weight ratio of the PA: DT: PES: photo initiator of the composition (PD31) was constant as 30:10:59:1 in all samples. Different content (2, 4, 8 wt% of solute) of fluorophore was added to PD31 to examine the effect of the fluorescent concentration on the patterning. The mixture was stirred and then filtered using membranes of 1.0 μm pore size attached to a Teflon syringe. The solution was coated on a slide glass with spacer and the resultant viscous film was dried under nitrogen flow for overnight to remove the solvent.

2.3. *Pattern Formation Using the Holographic Method*

Grating pattern was generated by a series of optical setup consisting of a diode laser (491 nm), polarizer, beam splitter, and detector, as reported before. To detect diffracted beam intensity during the holographic patterning in real time, a 635 nm-laser diode was used. A power ratio of the object and reference beams was fixed as 1:1 by the adjustable polarized beam-splitter (PBS), which is consists of a rotation half-wave plate, a polarizing beam-splitter cube, and a fixed half wave plate. The two beams were coherence on the photopolymer films and the interference pattern was generated at the films. The diffraction efficiency (η) was determined from the ratio of the diffraction intensity (ID) against the sum of ID and IT, where IT is the intensity of transmission beam.

2.4. *Characterization*

The average molecular weight of the fluorescent polymer was characterized by gel permeation chromatography (GPC) (model: Waters R-401 ALC/GPC) with THF as an eluent and polystyrene standard was used for calibration. Fluorescence spectrum of the film was obtained with luminescence spectrometer (Perkin–Elmer, Model LS55). The grating pattern image was examined by an optical microscopy (BH2-RFL-T3, Olympus Inc.) and a fluorescence microscopy.

3. Results and Discussion

The photopolymer films containing PMAn were photochemically active under the holographic patterning set up in Figure 2, to afford diffraction gratings. Figure 3 shows the diffraction efficiency (DE) increase of the 100 μm-thick film containing different content of fluorescent polyanthracene in PD31 composition during the holographic patterning. Diffraction efficiency of the PD31 film was increased within 100 s of patterning time, reaching a maximum value without fluorophore and showed maximum diffraction efficiency around 90%. In theory, the diffraction efficiency growth is proportional to the refractive index change (Δn) in the photopolymer film described in Eq. (1) [24].

$$\eta(\mathrm{t}) = \sin^2 \pi \Delta \mathrm{n}(\mathrm{t})\mathrm{T}/[\lambda_\mathrm{b} \cos(\theta_\mathrm{b})] \tag{1}$$

In our experiment, the film thickness (T) was 100 μm. The Bragg matched beam wavelength (λ_b) was 491 nm and Bragg angle of the probe beam (θ_b) was 15°. The refractive index change is affected by the monomer concentration ([M]), and diffusion coefficient (D) as described in Eq. (2). C_n is a constant [24].

$$\partial/\partial \mathrm{t}\ \mathrm{n}(\mathrm{x},\mathrm{t}) = \mathrm{C_n}\partial/\partial \mathrm{x}\ \mathrm{D}[\partial/\partial \mathrm{x}\ [\mathrm{M}]\ (\mathrm{x},\mathrm{t})] \tag{2}$$

Diffusion coefficient is generally dependent on the monomer concentration and on other physical characteristics of the material such as viscosity. In the presence of PMAn, the DE was reduced, possibly due to that the diffusion of monomers is blocked by the large fluorophore (PMAn).Thus the growth of DE is slow and the maximum DE value is decreased as the contents of PMAn is increased, as the D value in Eq. (2) is smaller for higher PMAn content. Similarly, the DE of the film containing high Mw PMAn (HPMAn) was much lower than that containing low Mw PMAn (LPMAn) as shown in Figure 3. The DE of the PMAn doped film with thickness of 100 μm was maximized to 50% with 2 wt% of LPMAn doping.

Absorption spectra of the photopolymer film showed in Figure 4. It showed clearly the increased absorption spectrum around the 415 nm ranges after adding

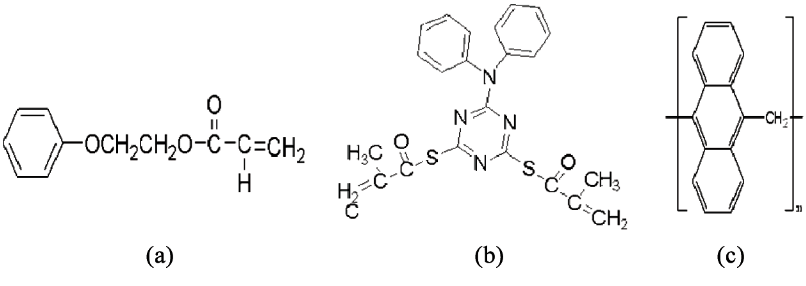

Figure 1. Structures of monomers (a) PA: Ethylene glycol phenyl ether acrylate (POEA), (b) DT: triazine dimethacrylate, and (c) poly(methyl anthracene) (PMAn).

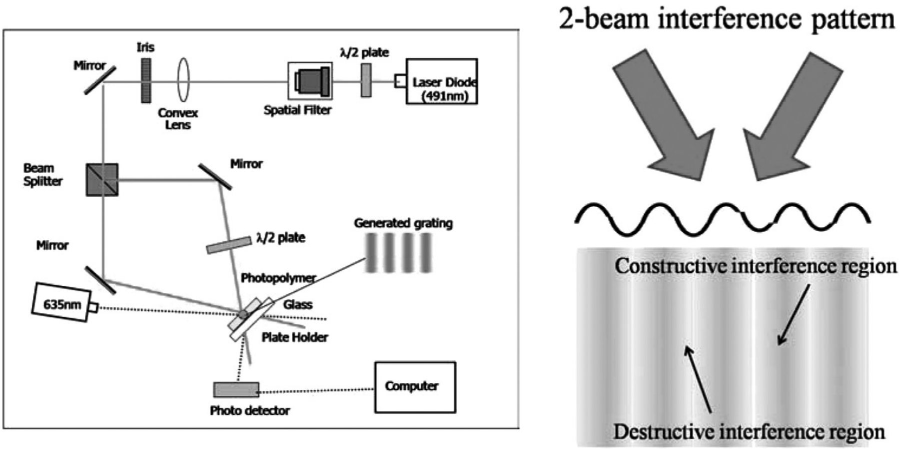

Figure 2. Schematics of the holography patterning set-ups and beam-profiles on the photopolymer surface.

the PMAn fluorophore to the photopolymer composite. Interestingly the fluorescence of the film after grating formation (exposed) was enhanced compared to the unexposed area. This result matched well to the previous report [25]. Thus such an enhancement could be ascribed to the micro separation between the fluorescent polymers by the grating patterns.

The emission maximum of the spectrum before and after holographic patterning was almost same for the same Mw fluorophore. Compared to the LPMAn, the HPMAn showed emission maximum at longer wavelength under the excitation wavelength of 415 nm [26].

The fluorescent spectra of the photopolymer film clearly showed the enhancement of the emission intensity after the patterning compare to the unpatterned area (Fig. 5). Interestingly, before patterning, the HPMAn film showed lower fluorescent intensity than the LPMAn film. This may be ascribed to that fluorescence intensity

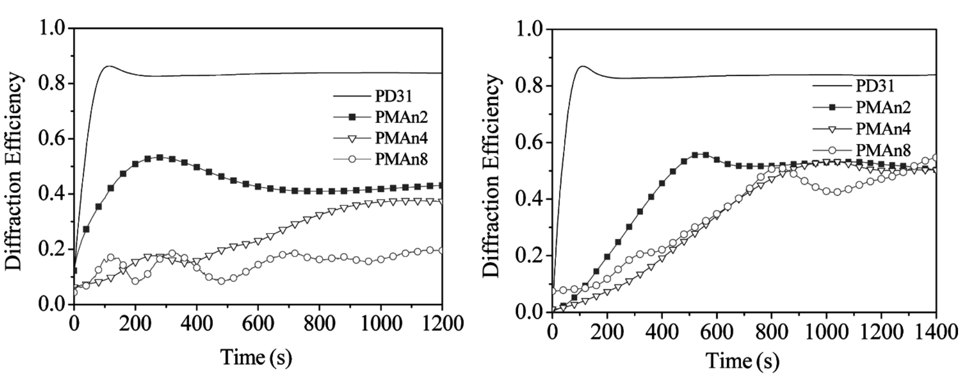

(a) (b)

Figure 3. Growth of the diffraction efficiency for the PMAn containing film: PMAn content of 0 wt% (solid line), 2 wt% (square), 4 wt% (triangle), and 8 wt% (circle) for PMAn of Mw.1225 (a) and 3650 (b). Thickness of the film was 100 μm.

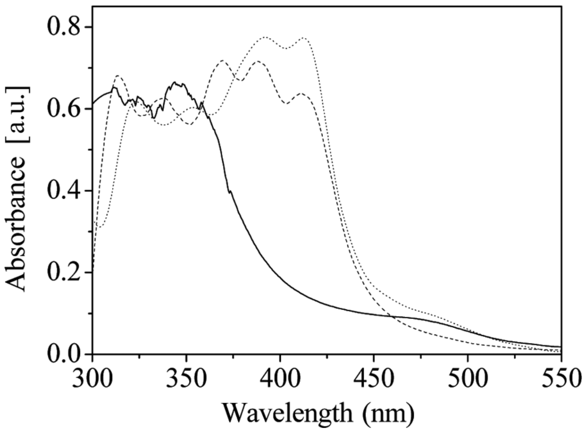

Figure 4. Absorbance spectra of the photopolymer film containing low Mw PMAn (average Mw = 1225, dot line) and high Mw PMAn (average Mw = 3650, dashed line) before patterning, as compared to that of film without PMAn (solid line).

of the high Mw PMAn was quenched more easily than the low Mw PMAn with neighboring molecules [27]. Surprisingly, after the patterning, the fluorescence intensity was more enhanced and the patterns were more clearly observed in the film with HPMAn than that with the LPMAn. The fluorescence contrasts, defined as R in Eq. (3), were determined as 7.02 and 2.46 for the film containing 2 wt% of HPMAn and LPMAn, respectively.

$$R = \text{fluorescence intensity of the recorded area/unrecorded area} \qquad (3)$$

This result could be ascribed to the separation of PMAn polymers during the monomer diffusion and thus reduce the possibility of excited quenching of the polymer by the neighboring polymers, as described before. The films with more than

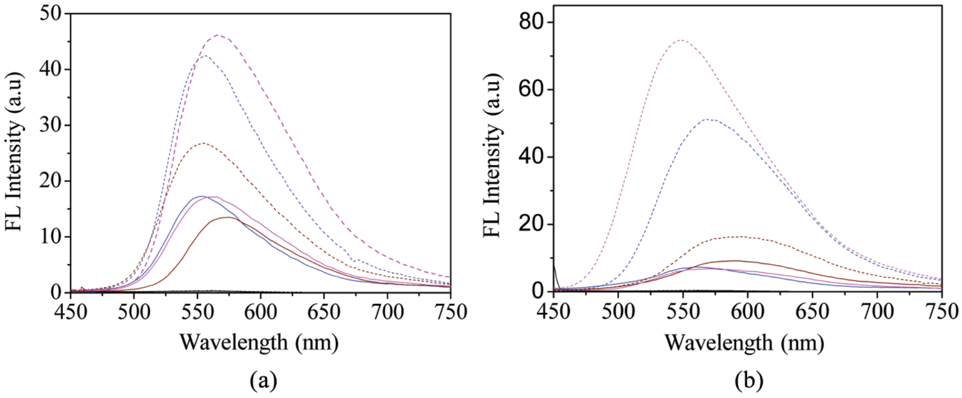

(a) (b)

Figure 5. Emission spectra of the photopolymers under 415 nm excitation, before (solid line) and after (dotted line) patterning for (a) low Mw PMAn (Mw = 1225) and (b) high Mw PMAn (Mw = 3650) containing different concentration of PMAn: 0 wt% (black), 2 wt% (blue), 4 wt% (wine), 8 wt% (magenta).

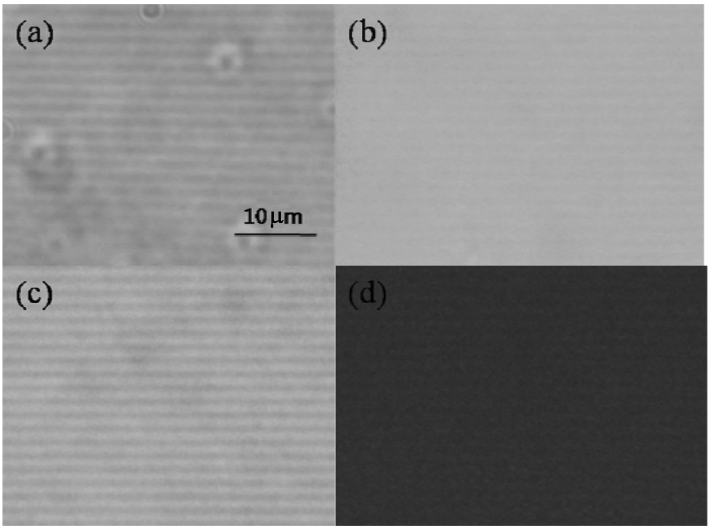

Figure 6. Pattern images on the HPMAn (2 wt%) film under the optical and fluorescent microscope. ($\theta_b = 15$), thickness 50 μm. (a) Optical microscope image, (b) green, (c) red, and (d) blue emission images.

4 wt% fluorophore contents show less fluorescent intensity enhancement compare to that with 2 wt%. As described above, the DE of the film with higher PMAn shows slower growth in DE and lower maximum DE, as the increased PMAn disturbs the diffusion of monomer. Therefore efficiency for the grating pattern generation is decreased at the high PMAn. On the other hands, the fluorescence intensity is increased with the fluorophore content [20].

The two effects must be compensated in the film of high PMAn content, where the diffusion of monomer (DT) is slow but fluorescent intensity is high, as shown in Figure 5. As the fluorescent intensity of the film was more increased in the recorded (grating) area, the fluorescent grating pattern became vivid even with naked eye. Interference beams are used for photoreaction of monomers to generate the patterns. The grating period was about ~0.95 μm by a 491 nm laser patterning. It can be calculated by θ_b, following the Bragg's law in Eq. (4),

$$\lambda = 2n_e d \sin(\theta_b) \tag{4}$$

where d is the interlayer distance in the [111] direction and θ_b is the Bragg angle, which is the half value of the incident angle. The effective refractive index (n_e) is independently determined according to the literature [28]. Figure 6 shows an optical and fluorescent microscope image of the fluorescent pattern. Interestingly, the fine grating patterns were observed in the magnified image to show a grating spacing of ~0.95 μm which matched to the theoretical value from Eq. (4). Blue and green emission image showed vivid fluorescent gratings.

4. Conclusion

Fluorescent grating pattern formation on a photopolymer film doped with PMAn was examined with a molecular composite of acrylic monomer and polyanthracene as a fluorophore. The grating formation efficiency (DE) was affected by the content and Mw of PMAn, specifically free fluorophore concentration in polymer composite. The emission maximum of high Mw PMAn (HPMAn) was more red-shifted than the low Mw PMAn (LPMAn). The fluorescence intensity of the grating area was enhanced after pattern formation, possibly due to micro separation within photopolymer matrix between the fluorescent polymers by the photochemically polymerized PA and DT domain, which may lower the possibility of excited quenching of PMAn with the neighboring PMAn. The Mw of PMAn affected the absorbance and fluorescence of the photopolymer. The high Mw PMAn (HPMAn) showed more fluorescence quenching effect before the patterning. However, the fluorescence of the pattern from the HPMAn film was enhanced more than that from the LPMAn film. The fluorescence contrast (R) between the patterned against unpatterned area were determined as 7.02 and 2.46 for the film containing 2 wt% of HPMAn and LPMAn, respectively.

Acknowledgment

This work was supported by the National Research Foundation (NRF) grant funded by the Korea government (MEST) through the Active Polymer Center for Pattern Integration (No. R11-2007-050-00000-0) and financial support of Seoul R&BD Program (10816).

References

[1] Campbell, M., Sharp, D., Harrison, M., Denning, R., & Turberfield, A. (2000). *Nature*, *404*, 53.

[2] Woltman, S. J., Eakin, J. N., & Craword, G. P. (2006). *Opt. Lett.*, *31*, 3273.

[3] Cho, Y. H., Shin, C. W., Kim, N., Kim, B. K., & Kawakami, Y. (2005). *Chem. Mater.*, *17*, 6263.

[4] Wochnowski, C., Cheng, Y., Meteva, K., Sugioka, K., Midorikawa, K., & Metev, S. (2005). *J. Opt.*, *7*, 493.

[5] Kim, E., Park, J., Shin, C., & Kim, N. (2006). *Nanotechnology*, *17*, 12, 2899.

[6] Lee, H., Sarwade, B., Kim, E., & Lee, S. (2006). *SPIE, Materials and Applications*, 6335, 63350R.

[7] Kim, E., Park, J., Cho, S. Y., Kim, N., & Kim, J. H. (2003). *ETRI J.*, *25*, 253.

[8] Kim, E. (2005). *J. Korean Society for Imaging Science*, *11*, 65.

[9] Rhee, U. S., Caulfield, H. J., Shamir, J., Vikram, C. S., & Paehi, E. G. (1993). *Opt. Eng.*, *34*, 1839.

[10] Hong, J. H., McMichael, I., Chang, T. Y., Christian, W., & Paek, E. G. (1995). *Opt. Eng.*, *32*, 2193.

[11] Rhee, U.-S., Caulfield, H. J., Shamir, J., Vikram, C. S., & Mirsalehi, M. M. (1993). *Opt. Eng.*, *32*, 1839.

[12] Pu, A. & Psaltis, D. (1996). *Appl. Optics*, *35*, 2389.

[13] Semenova, I. & Reinhand, N. (1998). IV, *T. J. Trout*, ed., Proc. SPIE 3294, 207.

[14] Zhao, C., Liu, J., Fu, Z., & Chen, R. T. (1997). *Appl. Phys. Lett.*, *71*, 1464.

[15] Schwider, J., Dresil, T., Beyerlein, M., Harder, I., Lindlein, N., Collischon, M., & Leuches, C. (2001). *Laser Opto.*, *33*, 41.

[16] Natansohn, A. & Rochon, P. (2002). *Chem. Rev.*, *102*, 4139.

[17] Oliveira, O. N., Li, L., Kumar, J., & Tripathy, S. K. (2002). In: *Photoreactive Organic Thin Films*, Sekkat, Z. & Knoll, K. (Eds.), Academic: San Diego, 429.

[18] Kim, E. (2007). Photorefractive Materials and Their Applications 2, Materials, Series: Springer Series in Optical Sciences Chap. 17.

[19] (a) Pietsch, U. & Rochon, P. (2003). *J. Appl. Phys.*, *94*, 963; (b) Lagugné- Labarthet, F., Brunel, J. L., Buffeteau, T., & Sourisseau, C. (2004). *J. Phys. Chem. B*, *108*, 6949; (c) Fiorini, C., Prudhomme, N., de Veyrac, G., Maurin, I., Raimond, P., & Nunzi, J.-M. (2000). *Synthetic. Met.*, *115*, 121.

[20] Oh, H., Kim, J., & Kim, E. (2008). *Macromolecules*, *41*, 19, 7160.

[21] Lee, H., Sarwade, B. D., & Kim, E. (2007). *Opt. Mater.*, *30*, 637.

[22] Rameshbabu, K., Kim, Y., Kwon, T., Yoo, J., & Kim, E. (2007). *Tetrahedron Lett.*, *48*, 4755.

[23] Oh, H., Kim, J., Rameshbabu, K., DO, J., & Kim, E. (2008). *J. Nanosci. Nanotechnol.*, *8*, 4616.

[24] Piazzolla, S. & Jenkins, B. K. (2000). *J. Opt. Soc. Am. B*, *17*, 7.

[25] Kim, J., Oh, H., Yoo, J., & Kim, E. (2008). *Mol. Cryst. Liq. Cryst.*, *491*, 67.

[26] Lo'pez Cabarcos, E. & Carter, Sue A. (2005). *Macromolecules*, *38*, 10537.

[27] Zhao, X., Jiang, H., & Schanze, K. S. (2008). *Macromolecules*, *41*, 3422.

[28] Lee, S. K., Park, S. G., Moon, J. H., & Yang, S. M. (2008). *Lab Chip*, *8*, 388.